A Dimension-Reduction Multibeam Antenna Scheme With Dual Integrated Butler Matrix Networks for Low-Complex Massive MIMO Systems

Yongjian Zhang and Yue Li, *Senior Member, IEEE*

***Abstract*—In this letter, a multiple-beam antenna (MBA) scheme with reduced port dimension is proposed for low-complex massive multiple-input–multiple-output (MIMO) systems. From practical scenario consideration, two 2-port and 8-element subarrays with dual 2-to-8 Butler matrix networks are designed for 3 dB beam coverage within 60° sector. Based on channel capacity analysis of an 8-subarray (8 × 8-element) antenna system, it is proved that only 25% number of radio frequency (RF) chains are utilized in the proposed scheme to achieve a competitive data transmission rate, compared with a regular 8 × 8-element and 64-chain massive MIMO system, with the advantages of low cost, low system weight, and low complexity of signal processing. The proposed 8-subarray system is built and measured to verify the antenna performance. The proposed multibeam antenna scheme exhibits potential possibilities in low-complex and low-cost massive MIMO systems for the fifth-generation (5G) applications.**

***Index Terms*—Antenna array, antenna diversity, antenna radiation patterns, Butler matrix networks, multiple-input–multiple-output (MIMO) antennas.**

I. Introduction

As ONE of the key technologies for the fifth-generation (5G) networks, massive multiple-input–multiple-output (MIMO) method is considered as an extension of conventional MIMO by utilizing more antennas [1], [2]. The massive MIMO attracts wide attention of researchers for its capability of achieving intensive beam coverage and increasing the channel capacity [3]. However, the implementation of a massive MIMO system will increase the number of radio frequency (RF) chains and the signal processing complexity logarithmically, resulting in the larger system size and weight, higher power consumption, and cost [4], [5]. Generally speaking, in a conventional MIMO system, each antenna connects with an RF chain, including amplifiers and other devices, introducing disastrous burden to the deployment of the base station (BS). Therefore, reducing the RF complexity of BS antenna systems becomes quite important in practical massive MIMO applications.

The multibeam antenna (MBA) is a feasible solution to reduce RF complexity in massive MIMO systems [6]. In the design of MBAs, the phase-shifting network plays a critical role in beamforming and determines the system cost and complexity. The quasioptics-based MBAs generate multiple beams by adopting the spatial retardation as a phase-shifting structure, such as the reflector-based [7]–[9] and the lens-based MBAs [10]–[12]. Inspired by the quasioptics phase shifting, the metasurface antennas utilize periodic elements in planar structures, i.e., meta-mirror or meta-lens, exhibiting extra freedom in phase control [13]–[19]. These types of MBAs usually apply the spatial-fed scheme, increasing the volume of BS. The active digital MBAs achieve specific phase distribution by employing digital processing chips, leading the challenges of computational resource and beamforming algorithms [20]–[22]. Besides, the MBAs based on Butler matrix are demonstrated in a compact and exquisite approach utilizing the beamforming circuit that is integrated with the antennas [23], [24], exhibiting potential possibilities for RF complexity reduction in practical massive MIMO systems.

In this letter, an integrated MBA scheme, with dual Butler matrix networks and four elevated beam clusters, is proposed for RF complexity reduction in massive MIMO systems. To achieve 3 dB beam coverage within elevation angle of 60° in the practical scenario, two types of integrated Butler matrix networks are designed in eight subarrays. Each subarray includes eight elements and only two input ports. It has been confirmed that the proposed MBA scheme with 8 × 8 elements and 16 RF chains is able to achieve the channel capacity comparatively closer to the conventional scheme with 8 × 8 elements and full 64 RF chains. Therefore, only 25% of RF chains are utilized in the proposed MBA scheme in low-complex massive MIMO systems for the 5G applications.

II. Dimension-Reduction Scheme

In some large-scale sites, i.e., rest area, both urban micro and macro cells are required for efficient spectrum utilization [25]. A practical line-of-sight (LoS) scenario with both urban micro and macro communication in massive MIMO system is considered to study the beam redundancy. As shown in Fig. 1, based on the 3GPP standard [26], [27], $h_{\mathrm{BS}} = 25$ m and $h_{\mathrm{UT}} = 1.5$ m are the heights of BS and mobile users, $r_{\max} = 500$ m and $r_{\min} = 10$ m

Manuscript received April 4, 2020; revised May 17, 2020; accepted June 8, 2020. Date of publication June 11, 2020; date of current version November 23, 2020. This work was supported in part by the Natural Science Foundation of Beijing Manipulate under Contract 4182029 and in part by the Youth Top Program of Beijing Outstanding Talent Funding Project. *(Corresponding author: Yue Li.)*

The authors are with the Department of Electronic Engineering, Tsinghua University, Beijing 100084, China, and also with the Beijing National Research Center for Information Science and Technology, Tsinghua University, Beijing 100084, China (e-mail: zhangyj18@mails.tsinghua.edu.cn; lyee@tsinghua.edu.cn).

Digital Object Identifier 10.1109/LAWP.2020.3001565

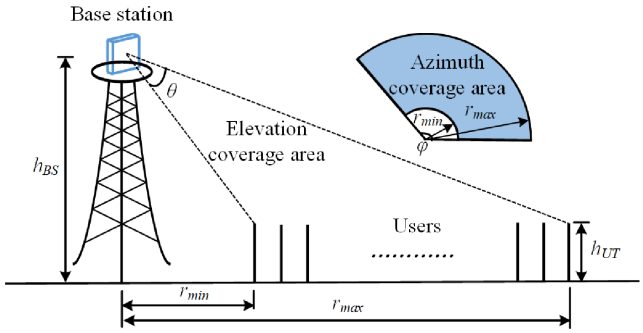

Fig. 1. Practical communication scenario in massive MIMO systems.

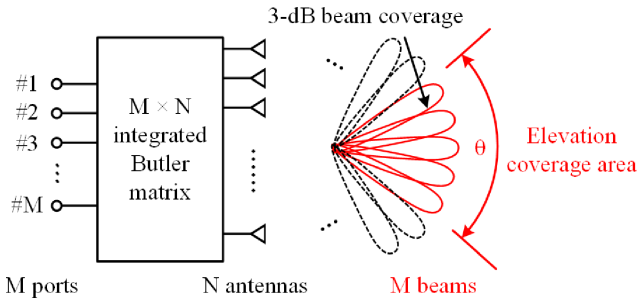

Fig. 2. Diagram of the proposed multibeam scheme.

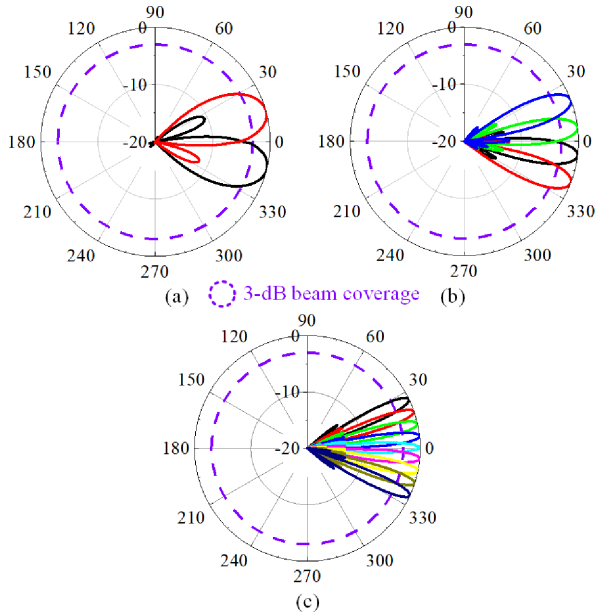

Fig. 3. Normalized radiation patterns of different dimension-reduction schemes in coverage area, where N is the element number and M is selected beam number. (a) $M = 2, N = 4$. (b) $M = 4, N = 8$. (c) $M = 9, N = 16$.

TABLE I
DETAILED DIMENSIONS (UNIT: mm)

l_1	l_2	l_3	l_4	l_5	l_6	l	w	w_1	g_1	g_2	d
22	29	32	12.4	25	174.4	470	214.4	7.8	2	2.6	58

denote the longest and nearest distance between BS and mobile users, $\varphi = 120°$ and $\theta = 60°$ are the azimuth and elevation coverage angle of users. Apparently, the signals in uplink and downlink between BS and users are mainly transmitted within the angle θ in elevated plane, indicating that the antenna beams at other angles, i.e., $360°-\theta$ is redundant for communication.

From the consideration of RF complexity reduction, the MBAs based on Butler matrix networks are presented for beam selection, as shown in Fig. 2. In the proposed scheme, M out of N beams are selected to achieve pertinent 3 dB beam coverage in the elevation angle θ, and thus, $N - M$ RF chains are terminated for complexity reduction.

Antenna arrays with different element numbers are presented in Fig. 3. Considering the 3 dB beam coverage for practical communication, a proper number of beams are selected to achieve the user coverage. For example, there are four antenna elements and two beams selected, and we name it as 2-out-of-4 scheme. In the schemes in Fig. 3, the performance of 4-out-of-8 MBAs scheme is more appropriate, while 2-out-of-4 scheme has an inferior gain due to the small number of antenna elements and 9-out-of-16 scheme is with high complexity of feeding networks due to the large number of selected beams. To further reduce the number of RF chains, a 4-to-8 Butler matrix network is correspondingly divided into dual 2-to-8 Butler matrix networks. Therefore, two types of 2-to-8 integrated Butler matrix networks are utilized in the proposed scheme.

III. ANTENNA ARRAY DESIGN

The general idea of the proposed MBA scheme is denoted in Fig. 4(a). The whole antenna array consists of 8 × 8 elements, which are divided into eight subarrays. These subarrays are also divided into blue and red groups with different Butler matrix networks named as type A and type B, as shown in Fig. 4(a). Each subarray is connected with a 2-to-8 integrated Butler matrix network. Thus, only 25% of RF chains are used, enormously reducing the RF complexity of system.

The diagrams of two types of Butler matrix networks are shown in Fig. 4(b) and (c), respectively. Type A Butler matrix network consists of two input ports, four 22.5° and two 45° delay lines (as phase shifters), four hybrid couplers, six crossovers, and eight output ports connecting with eight antenna elements. Two opposite gradient phase distributions are achieved in the antenna elements when fed through port A (green) and port B (purple), generating dual beams steering at ±7°. The integrated Butler matrix network is fabricated on both sides of a print circuit board with solid lines on the front side and dash lines on the back side in Fig. 4(b). The detailed structure of the 2-to-8 Butler matrix network with eight dipole antenna elements is shown in Fig. 5, and the value of each parameter is listed in Table I. Type B Butler matrix network utilizes four 67.5° and two 135° delay lines as phase shifters, with other structures the same as Type A. Therefore, ±21° beams are achieved through port C (blue) and port D (red).

An 8 × 8-element MBA array is built with four type A and four type B Butler matrix networks, generating four beam clusters at ±7° and ±21°, as shown in Fig. 4(a). For each beam cluster, four ports in the corresponding group are cooperatively phase-tuned

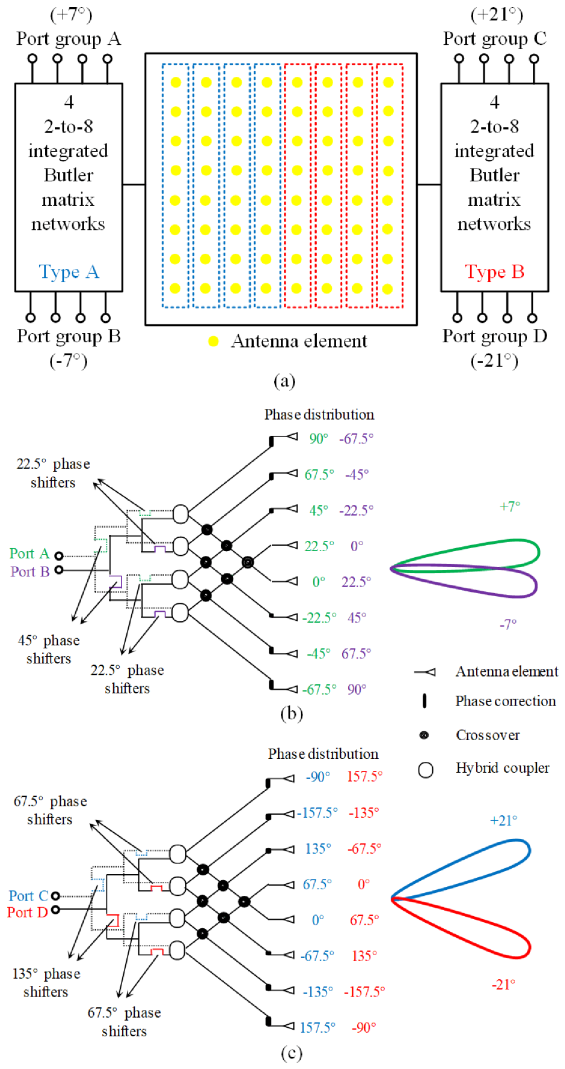

Fig. 4. Proposed scheme implementation framework. (a) Schematic diagram of the proposed antenna array. Diagrams of two integrated Butler matrix networks: (b) type A; (c) type B.

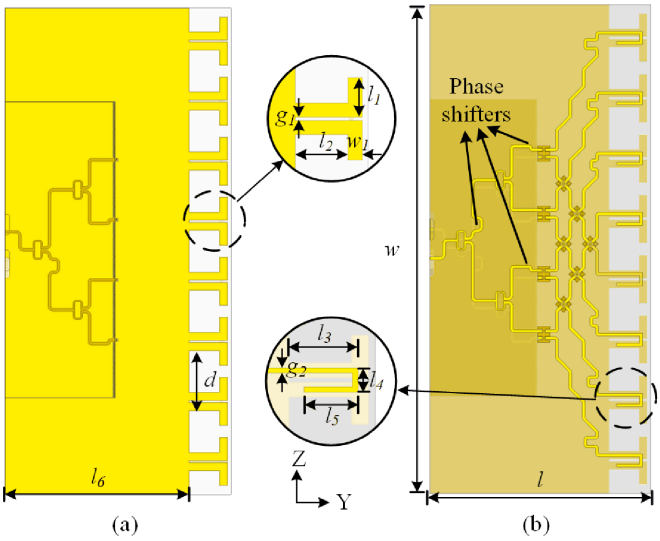

Fig. 5. Simulated model of the proposed type A subarray with two ports and eight antenna elements. (a) Front view. (b) Back view.

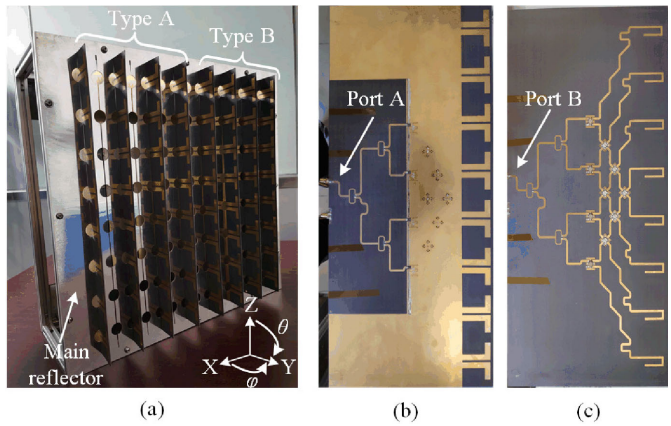

Fig. 6. Photographs of the antenna array using the proposed MBA scheme. (a) 8 × 8-element array. Photographs of the proposed type A subarray. (b) Front view. (c) Back view.

to generate the beam clusters for multiple users and steer in the azimuthal plane. As a result, two-dimensional beam scanning can be achieved, with the beam selection in elevated plane and dynamic amplitude or phase adjustment in azimuthal plane. In the whole design, 16 input ports and 64 antenna elements are integrated with eight Butler matrix networks as eight subarrays, and 16 RF chains are needed for four beam clusters with 60° 3 dB elevated-plane coverage.

IV. Results

A prototype of the MBA array using the proposed scheme is fabricated and tested to demonstrate the design strategy, as shown in Fig. 6. The whole antenna array is supported by an aluminum shelf with a size of 522 × 214.4 × 510 mm^3. The subarrays with hybrid couplers (Anaren Xinger 1P603AS) and crossovers (Anaren Xinger X2BS) are constructed on an F4B substrate ($\varepsilon_r = 2.65$), as shown in Fig. 6(b) and (c), and located at half-wavelength distance between two adjacent ones. The usage of these two components would reduce the subarray gain by less than 2 dB and result in a small amount of phase error, which is compensated by the several delay lines between the Butler matrix networks and antenna elements. The measured *S*-parameters of subarray with the type A Butler matrix network are shown in Fig. 7, while the simulated results cannot be given because the hybrid couplers and crossover chips are unable to be modeled by the simulation software Ansoft HFSS. Fig. 7 illustrates the performance of impedance matching and port isolation of a subarray. The radiation patterns in *E*-plane of the proposed type A and B subarrays are shown in Fig. 8. The measured results (scatter dots) without reflector agree well with the simulated ones (dash lines), which are given without the Butler matrix networks due to the modeling restriction. However, there are several strong back lobes, resulting in the deterioration of front-to-back ratio performance. To suppress backward radiation, a planar metal reflector is adopted as the main reflector, perpendicular to the antenna elements and located l_6 away from the feeding ports. The simulated radiation patterns

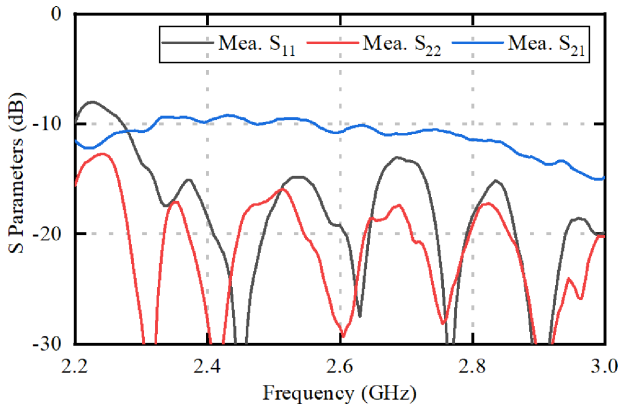

Fig. 7. *S*-parameters of the subarray with type A Butler matrix network.

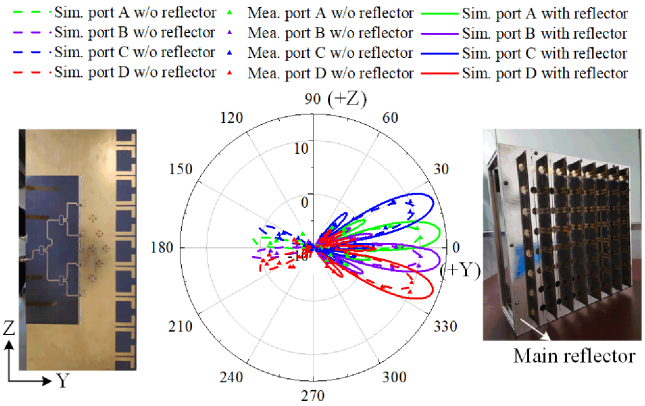

Fig. 8. Radiation patterns in *E*-plane of the proposed antenna subarray under measurement and simulation at 2.6 GHz.

(solid lines) show that the front-to-back ratio is improved by more than 20 dB through the usage of reflector, and with no obvious effect to the shape of main beam. The radiated results illustrate that the subarrays achieve four beams at $\pm 7°$ and $\pm 21°$ when fed through ports A to D, respectively. The 60° elevated sector coverage is achieved under the premise of pledging 3 dB beam level. The radiation patterns of the whole antenna array cannot be measured because it is too heavy to be supported by the turntable in the chamber, while there is little difference between the normalized radiation patterns of the subarray and whole array due to the high isolation among the subarrays. Therefore, the simulated results of two types of subarrays with main reflector are utilized in the following calculation of channel capacity.

To further study the performance of proposed scheme, we adopt a 3-D channel model based on Fig. 1. The mobile users are assumed uniformly distributed in the coverage area and six multipaths are assumed between the BS and the mobile user. Fig. 9 illustrates the calculated channel property based on the above multiuser scenario. Three schemes are involved in the discussion of channel capacity. Scheme 1: Eight beam clusters generated by the array with 8×8 elements, 8×8 ports with 64 RF chains, using eight 8-to-8 Butler matrix networks; Scheme 2: Four beam clusters generated by the array with 8×8 elements, 2×8 ports with 16 RF chains, using eight 2-to-8 Butler matrix

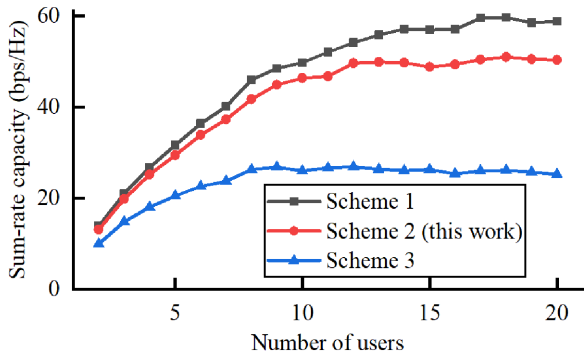

Fig. 9. Sum-rate capacity comparison between the proposed scheme and other traditional schemes.

networks (four types A and types B); Scheme 3: Two beam clusters generated by the array with 8×8 elements, 2×8 ports with 16 RF chains, using eight 2-to-8 type A Butler matrix networks (no type B used). The sum-rate capacity comparison among different schemes is shown in Fig. 9. 1) Comparison between Scheme 1 and Scheme 2: The calculated capacity difference is small, i.e., less than 2.8 bps/Hz, when the number of users (NU) is less than 8. When NU exceeds 15, the capacity saturates to be stable, and the difference between two schemes is 8.5 bps/Hz. Therefore, when NU is small, the capacity performance of Scheme 2 is similar to Scheme 1. For large NU value, Scheme 2 is with 85% of channel capacity but using only 25% number of RF chains, compared with Scheme 1. 2) Comparison between Scheme 2 and Scheme 3: As NU increases, the difference between two schemes becomes striking. When NU is more than 8, the sum-rate capacity of Scheme 3 saturates, with the value of 26 bps/Hz, due to the smaller coverage angle. We can see that the sum-rate capacity of Scheme 3 is only 48% of Scheme 2 but with the same number of RF chains. This is because 60° sector coverage in elevated plane can be achieved in the Scheme 2, while only a coverage area of 30° for Scheme 3, resulting in the poor channel performance in uncover area. Based on the comparison, Scheme 2, i.e., the proposed scheme, is with the best performance by considering the tradeoff between RF chain numbers and sum-rate capacity.

V. Conclusion

In this letter, an MBA scheme with low RF complexity is proposed for massive MIMO systems. A practical LoS scenario is adopted and discussed for verifying the large spatial beam redundancy due to the uniformed user distribution. Therefore, an 8×8-element antenna array with only 16 RF chains is designed for the sector coverage of multiusers. The measurement results show that the antenna array can realize four beam clusters within the user coverage area. Compared with the conventional scheme with 8×8 elements and 64 RF chains, the antenna array using the proposed scheme achieves an approaching sum-rate channel capacity, but only 25% of RF chains are utilized. As a result, the proposed MBA scheme is with the merits of compact volume and low RF complexity, exhibiting valuable potentials in 5G massive MIMO applications.

REFERENCES

[1] J. G. Andrews *et al.*, "What will 5G be?," *IEEE J. Sel. Areas Commun.*, vol. 32, no. 6, pp. 1065–1082, Jun. 2014.

[2] A. Gupta and R. K. Jha, "A survey of 5G network: Architecture and emerging technologies," *IEEE Access*, vol. 3, pp. 1206–1232, 2015.

[3] J. Zhang, S. Chen, Y. Lin, J. Zheng, B. Ai, and L. Hanzo, "Cell-free massive MIMO: A new next-generation paradigm," *IEEE Access*, vol. 7, pp. 99878–99888, 2019.

[4] L. Lu, G. Y. Li, A. L. Swindlehurst, A. Ashikhmin, and R. Zhang, "An overview of massive MIMO: Benefits and challenges," *IEEE J. Sel. Topics Signal Process.*, vol. 8, no. 5, pp. 742–758, Oct. 2014.

[5] G. Yu, X. Chen, and D. W. K. Ng, "Low-cost design of massive access for cellular Internet of Things," *IEEE Trans. Commun.*, vol. 67, no. 11, pp. 8008–8020, Nov. 2019.

[6] W. Hong *et al.*, "Multibeam antenna technologies for 5G wireless communications," *IEEE Trans. Antennas Propag.*, vol. 65, no. 12, pp. 6231–6249, Dec. 2017.

[7] A. Neto, M. Ettorre, G. Gerini, and P. De Maagt, "Leaky wave enhanced feeds for multibeam reflectors to be used for telecom satellite based links," *IEEE Trans. Antennas Propag.*, vol. 60, no. 1, pp. 110–120, Jan. 2012.

[8] A. Young, M. V. Ivashina, R. Maaskant, O. A. Iupikov, and D. B. Davidson, "Improving the calibration efficiency of an array fed reflector antenna through constrained beamforming," *IEEE Trans. Antennas Propag.*, vol. 61, no. 7, pp. 3538–3545, Jul. 2013.

[9] Y. J. Cheng, W. Hong, and K. Wu, "Millimeter-wave substrate integrated waveguide multibeam antenna based on the parabolic reflector principle," *IEEE Trans. Antennas Propag.*, vol. 56, no. 9, pp. 3055–3058, Sep. 2008.

[10] H. Chou and Z. Yan, "Parallel-plate Luneburg lens antenna for broadband multibeam radiation at millimeter-wave frequencies with design optimization," *IEEE Trans. Antennas Propag.*, vol. 66, no. 11, pp. 5794–5804, Nov. 2018.

[11] A. B. Numan, J. Frigon, and J. Laurin, "Printed W-band multibeam antenna with Luneburg lens-based beamforming network," *IEEE Trans. Antennas Propag.*, vol. 66, no. 10, pp. 5614–5619, Oct. 2018.

[12] Y. Li, L. Ge, M. Chen, Z. Zhang, Z. Li, and J. Wang, "Multibeam 3-D-printed Luneburg lens fed by magnetoelectric dipole antennas for millimeter-wave MIMO applications," *IEEE Trans. Antennas Propag.*, vol. 67, no. 5, pp. 2923–2933, May 2019.

[13] J. P. S. Wong, A. Epstein, and G. V. Eleftheriades, "Reflectionless wide-angle refracting metasurfaces," *IEEE Antennas Wireless Propag. Lett.*, vol. 15, pp. 1293–1296, 2016.

[14] O. Quevedo-Teruel, M. Ebrahimpouri, and M. Ng Mou Kehn, "Ultrawideband metasurface lenses based on off-shifted opposite layers," *IEEE Antennas Wireless Propag. Lett.*, vol. 15, pp. 484–487, 2016.

[15] M. Chen, A. Epstein, and G. V. Eleftheriades, "Design and experimental verification of a passive Huygens' metasurface lens for gain enhancement of frequency-scanning slotted-waveguide antennas," *IEEE Trans. Antennas Propag.*, vol. 67, no. 7, pp. 4678–4692, Jul. 2019.

[16] K. Srivastava *et al.*, "Wideband and high-gain circularly polarised microstrip antenna design using sandwiched metasurfaces and partially reflecting surface," *Microw., Antennas Propag.*, vol. 13, no. 3, pp. 305–312, Feb. 2019.

[17] D. González-Ovejero, G. Minatti, G. Chattopadhyay, and S. Maci, "Multibeam by metasurface antennas," *IEEE Trans. Antennas Propag.*, vol. 65, no. 6, pp. 2923–2930, Jun. 2017.

[18] L. Boccia, I. Russo, G. Amendola, and G. Di Massa, "Multilayer antenna-filter antenna for beam-steering transmit-array applications," *IEEE Trans. Antennas Propag.*, vol. 60, no. 7, pp. 2287–2300, Jul. 2012.

[19] J. Wang *et al.*, "Metantenna: When metasurface meets antenna again," *IEEE Trans. Antennas Propag.*, vol. 68, no. 3, pp. 1332–1347, Mar. 2020.

[20] P. Xingdong, H. Wei, Y. Tianyang, and L. Linsheng, "Design and implementation of an active multibeam antenna system with 64 RF channels and 256 antenna elements for massive MIMO application in 5G wireless communications," *China Commun.*, vol. 11, no. 11, pp. 16–23, Nov. 2014.

[21] H. Al-Saedi *et al.*, "An integrated circularly polarized transmitter active phased-array antenna for emerging ka-band satellite mobile terminals," *IEEE Trans. Antennas Propag.*, vol. 67, no. 8, pp. 5344–5352, Aug. 2019.

[22] S. Moon, S. Yun, I. Yom, and H. L. Lee, "Phased array shaped-beam satellite antenna with boosted-beam control," *IEEE Trans. Antennas Propag.*, vol. 67, no. 12, pp. 7633–7636, Dec. 2019.

[23] F. Y. Xia, Y. J. Cheng, Y. F. Wu, and Y. Fan, "V-band wideband circularly polarized endfire multibeam antenna with wide beam coverage," *IEEE Antennas Wireless Propag. Lett.*, vol. 18, no. 8, pp. 1616–1620, Aug. 2019.

[24] Y. J. Cheng, W. B. He, C. X. Weng, and Y. Fan, "Frequency-agile Butler matrix with good interference suppression for multiple radio wireless platforms," *Microw., Antennas Propag.*, vol. 7, no. 7, pp. 563–568, May 2013.

[25] H. Asakura and T. Fujii, "Combining micro and macro cells in a cellular system," in *Proc. IEEE Int. Conf. Universal Pers. Commun.*, vol. 2, 1993, pp. 728–731.

[26] 3GPP. "Study on 3D channel model for LTE," Tech. Rep. TR36.873, V12.1.0, Mar. 2015.

[27] 3GPP, "Study on channel model for frequencies from 0.5 to 100 GHz," Tech. Rep. TR38.901, V15.0.0, Jun. 2018.